Title: Effect of Parenchymal Arachnoid on Brain Fluid Transport

Running Title: Effect of Parenchymal Arachnoid on Brain Transport

Authors: Eric Hansen[1,*], Christopher Janson[2], Liudmila Romanova[3], Cornelius H. Lam[4]

1. *Department of Neurosurgery, Minneapolis Veterans Administration Health Care System, United States.*
2. *Internal Medicine and Neurology, Wright State University, Beavercreek, OH, USA.*
3. *Department of Neurology and Rehabilitation, University of Illinois, Chicago, IL, USA.*
4. *Department of Neurosurgery, University of Minnesota, Minnesota.*

***Corresponding Author**: Eric Hansen, Department of Neurosurgery, Minneapolis Veterans Administration Health Care System, United States. Email: hanse989@umn.edu

To appear in: **Basic and Clinical Neuroscience**

Received date: 2020/11/30

Revised date: 2021/11/10

Accepted date: 2022/06/27

Please cite this article as:

Hansen, E., Janson, C., Romanova, L., & Lam, C. H. (In Press). Effect of Parenchymal Arachnoid on Brain Fluid Transport. *Basic and Clinical Neuroscience*. Just Accepted publication Aug. 15, 2022. Doi: http://dx.doi.org/10.32598/bcn.2022.3089.1

DOI: http://dx.doi.org/10.32598/bcn.2022.3089.1

Abstract

***INTRODUCTION**:*

The pia-arachnoid is a critical component of cerebrospinal fluid removal. It covers and invaginates into brain parenchyma and physiologic failure results in hydrocephalus and cerebral edema. The purpose of this study was to characterize the role of arachnoid within brain parenchyma and determine if water flux and solute transport is affected by these intra-parenchymal cells.

***METHODS**:*

An immortalized arachnoid rat cell line was used to seed *300 µm* organotypic rat brain slices of 4-week old rats. Fluid and tracer transport analyses were conducted following a 7-10 day intraparenchymal growth period. The development of an arachnoid brain slice model was characterized using diffusion chamber experiments to calculate permeability, diffusion coefficient, and flux.

***RESULTS**:*

Labeled rat arachnoid cells readily penetrated organotypic cultures for up to 10 days. A significant reduction of dye and water flux across arachnoid impregnated brain slices was observed after 3 hours in the diffusion chamber. Permeability decreased in whole brain slices containing arachnoid cells compared to slices without arachnoid cells. While a significant reduction of dextran across all slices occurred when molecular weights increased from 40 kDA to 70kDA.

***CONCLUSION**:*

Tracer and small molecule studies show that the presence of arachnoid cells have a significant impact on the movement of water through brain parenchyma. Size differential experiments indicate that between 40 and 70 kDa, the permeability of solute changed substantially, which is an important marker of blood-CSF barrier definition. We have developed an arachnoid organotypic model that reveals their ability to alter permeability and transport.

Keywords: Arachnoid, Organotypic cell culture, Permeability, Diffusion, Parenchyma

Introduction

The arachnoid-pial membrane forms a physical barrier over the surface of the brain, which delimits blood and other substances and is an important component of cerebrospinal fluid (CSF) flow.[1,2] The pia-arachnoid also invaginates deep into the brain following blood vessels and grows into the parenchyma during development.[3] It has been hypothesized that the pia and the arachnoid have the same embryologic origin, both derived from an ectodermal origin the perimedullary mesenchyme.[4] Forming thin sheaths that occupy the Virchow-Robin spaces, leptomeninges line the small vessels responsible for the blood brain barrier (BBB). While extra-parenchymal arachnoid granulation physiology has been explored in detail in the past, questions about parenchymal arachnoidal contribution to brain transport is unclear.[5] A better understanding of water flux in brain tissue is important in many pathologic conditions including trauma, tumor growth, and brain edema, and the pia-arachnoid along with the ependyma are the two critical components of the brain-CSF interface.[5-7]

How fluid and solute flux occurs at the pia-arachnoid barrier between the subarachnoid space and CSF remains an open question, and the extent of leptomeningeal barrier function at the interface between brain parenchyma and CSF is also poorly understood.[8] In arachnoid tissue, tight junctions and other paracellular adhesions are the predominant component of the blood-CSF-barrier (BCB). Previous studies have shown that arachnoid cells form tight junctions within 5-7 days on 2-dimensional cultures.[9,10] The tight junctions and extracellular matrix derived from arachnoid, are key components in delimiting neuro-transport.[11-13] Downstream effects of transport disruption includes alterations in neighboring cell communications, function, and pathologic spread of disease.

We present a new model to determine arachnoids' effects on brain parenchyma using whole brain slices. Studying parenchymal arachnoid cells is challenging due to their proximal location to blood vessels. Arachnoid tissue can be difficult to isolate, culture, and track in-situ and determining their function within brain parenchyma can also be technically demanding. We have found no other studies that have attempted to examine the role of arachnoid in this location. While taking advantage of our robust cell lines, our initial whole brain slice approach mitigates the problem of observing cells out of their environment in isolation. We began by populating organotypic cultures with leptomeningeal cells, to determine the viability of this model. Secondly, we examined whether transport through parenchyma is affected by the seeded arachnoid cells. With these cells interdigitating into the brain, our hypothesis is

that fluid and tracer transport is altered due to paracellular and transcellular effects. This model of deeply embedded arachnoid is currently the closest mimic of their function within brain parenchyma.

Materials and Methods

Brain Slice Preparation:

Sprague Dawley Rats (approximately 4 weeks old) were rapidly sacrificed (CO_2 and decapitation). A total of 18 rats were used. The brains were removed and glued with cyanoacrylate to the chuck of a water-cooled Leica VT1000A vibratome and trimmed with a razor. Under aseptic conditions, 300-µm-thick whole-brain coronal sections were cut and collected in sterile medium. The organotypic slices were carefully placed on a 3.0-µm membrane insert (Millipore Sigma Corning Transwell Cat # CLS3492) in 6-well plates. Arachnoid cells grown separately in culture plates were labelled with CellTracker™ (Thermofisher Cat # CM-Dil C7000) and incubated at 37 °C in humidified atmosphere of 95% air and 5% CO_2 in culture media containing Eagle's MEM with 10% fetal bovine serum (FBS) (Millipore Sigma Cat # F2442), nonessential amino acids (Millipore Sigma), glutamine (BioWhittaker Inc., Walkersville, MD), streptomycin, and penicillin (Millipore Sigmaaldrich Cat # P4333) at 10 µl/cc each. Medium was changed twice per week. 4×10^4 arachnoid cells were trypsinized and centrifuged at 3000 rpm for 3 minutes; the resulting pellet was homogenized and seeded with media solution on top of each brain slice. The arachnoid cells labelled with CellTracker™ was designed to display fluorescence to daughter cells but not adjacent cells in the population. Brain slices (1 per well), with the addition of arachnoid cells, were cultured at 37 °C and 5% CO_2. and incubated for up to 10 days with the medium changed twice per week. After three, seven, and ten days, membranes with brain slice were fixed in 10% formalin, and monitored for arachnoid cell growth and examined for apoptosis respectively. The other brain slices were carefully placed and sealed in the Permegear Side-bi- Side© chambers for permeability measurements.

Arachnoid cell line

We used our previously developed immortalized arachnoid rat cell line harvested from three week old Sprague-Dawley rats, which we established have barrier properties characteristic of the CSF-blood barrier.[12,14] Arachnoid cells were immortalized by BABE puro-SV40LT as previously described.[14] Briefly, clarified viral supernatant containing pBABE-puro-SV40LT was applied to the arachnoid cell primary culture. Target cells were initially at a density of 4_104 cells/well of a six-well plate. Media was aspirated and 3 ml virus-containing media was added per well. Polybrene (Cat # TR-1003 Millipore) was added to a final concentration of 4_g/ml. After 12–18 h of incubation, virus-containing media was aspirated and

replaced with fresh media, to avoid polybrene toxicity and possible adverse effects from conditioned media. Cells transduced with pBABE-puro-SV40LT were selected over 14 days with puromycin. To establish cell phenotype cells were stained with cytokeratin 18 antibody (Prod # C-04, Abcam Inc.), vimentin (Prod #080552; Invitrogen), and desmoplakin I + II (Prod # ab106342, Abcam, Inc.). Double labeling of vimentin and desmoplakin was done to verify cell identification.

To verify purity of the arachnoid cell isolations, cells were stained for the presence of potential contaminating cells: muscle, fibroblasts, endothelial cells, glial cells, and neuronal cells. Myosin (Prod # MA1-35718; Fisher Sci.) was used to identify muscle cells; S100 (Prod # 13E2E2; BioGenex) and glial fibrillary acidic protein (GFAP, G-A-5; Cell Marque) were used to identify glial cells; CD31 (1A10; Cell Marque) was used to identify endothelial cells; smooth muscle actin (SMA asm-1; Novacastra) was used to identify fibroblasts; neuronal nuclei (Prod # NeuN, MAB377; Millipore) was used to identify neuronal cells. Staining levels for the cells were compared to positive controls

Arachnoid cell growth and apoptosis on brain slices

To determine if arachnoid cells cultured on brain slices survived and penetrated organotypic slices, 3 brain slices were fixed in 10% formalin at each time point (i.e. day 3,7 and 10) and analyzed using a Biorad MRC-1024 single photon confocal microscope 1024 (Biorad Cell Science, UK). A total of 30 slices taken at 25µm increments from brains were viewed at each time point. All slices examined confirmed arachnoid cell survivability within the organotypic brain slice. To determine the extent of apoptosis of arachnoid cells grown on brain slices compared to standard culture plates, control cells were seeded on two 12-Transwell membrane plates and grown to confluency (>2 × 10^5 cells per well) for up to 10 days. At each time point media was removed, cells were washed ×2 with cold PBS, and rinsed in Binding Buffer. FITC Annexin V and Propidium Iodide was added according to the manufacturer's instructions (FITC Annexin V Apoptosis Detection Kit, BD Pharmingen, San Diego, CA). Relative frequencies of apoptosis of cells grown on Transwells compared to brain slices were determined by measuring absorbance at the 455 nm wavelength.

Growth constant calculations

Randomly selected cultures (n=3) were selected to measure growth, whose curve is described by equation 1.

1) $\ln (N_2/N_1) = k (t_2-t_1)$

Where N_1 equal the number of cells present in the population at time t_1 and N_2 equals the number of cells present at time t_2, and k is a growth constant that is specific for the population. During the exponential growth phase, k can be written as:

2) $k = \ln 2/t_D$

Where t_D = generation or doubling time.

Diffusion and Permeability Measurements

Dye experiments:

To test the diffusion rate of brain slices implanted with arachnoid cells, a Permegear side-bi-side chamber (PermeGear, Inc. 3.4 mL chamber, Hellertown, PA) was used. Controls of brain slices grown with fibroblast (n=6) and brain slices alone (n=6) were used. Temperature was maintained at 37°C and a brain slice placed on a 3.0 µm porous membrane. The membrane and brain (n=6 for each treatment) was carefully sealed between the chambers. At the start of experiment, Indigo Carmine (Millipore Sigma Cat #73436, St Louis, MO) diluted 1:10 was added to the donor chamber. At 10-minute intervals, 20 microliters samples were taken from the receiver chamber and the concentration of the dye (as a percentage of the donor compartment) was determined using a Packard SpectraCount photometric microplate reader (Packard Instrument Co., Meriden, CT).

A quantitative analysis of Indigo Carmine diffusion across organotypic slices was conducted using Fick's law. Diffusion (D) was calculated using equation 3:

3) $D = -\Phi / (c_1 - c_2 / x_1 - x_0)$

Where $(c_1 - c_2 / x_1 - x_0)$ is the concentration gradient. The number of moles that passes a certain plane per second is the net flow (Φ). D is the diffusion constant that is defined as the amount of a substance (in Mol) that diffuses through an area (cm^2) at a concentration gradient of 1 (Mol/cm).

Water Flux Experiments

To test water flux of brain slices implanted with arachnoid cells under 4 and 8 cm pressure gradients, the diffusion chamber was fitted with a manometer. Applying a hydraulic pressure difference of 4 and 8 cm H_2O over a 2h time period allowed us to measure the volumetric flow rate (J_v) under differences in pressure (n=6 for each pressure). The displacement of water was tracked and converted to J_v according equation 4:

4) $J_v = (\Delta d/\Delta t) \times F$

where $\Delta d/\Delta t$ is the displacement rate and *F* is a tube calibration factor (fluid volume occupying a known length of tubing). Because each chamber contained the same medium (DMEM), there was no osmotic pressure difference across the cell layer. Flux was obtained by measuring the volume of water displaced in the donor compartment per cm^2/s.

Dextran Experiments

For large molecule transport studies, FITC labeled Dextran, of sizes 10, 40, 70, and 150 kilodaltons (Sigma-Aldrich Co., St. Louis, MO) were placed in the donor compartment of the diffusion chamber (n=6 for each size). Briefly, Dextran was dissolved in warm HBSS (Hank's balanced salt solution; including NaHCO3 at .33g/L with HEPES buffer (0.01M)) which produced 2.5 mg/mL of test solutions. The initial concentration of Dextran was obtained by sampling the donor chamber at time 0. Samples of 100ul were taken from the receiving chamber every 30 minutes for 6 hours to calculate permeability. Samples were placed on a 96-well plate and 100 µL of 40 mg/mL NaOH aqueous solution added to each sample. Fluorescence was measured via excitation and emission wavelengths of 485 and 530 nm, respectively. All signals were measured using a Packard SpectraCount© photometric microplate reader (Packard Instrument Co., Meriden, CT) with control plates subtracted out.

The apparent in vitro permeability coefficient (P_{app}) was determined using equation 5:

5) $$P_{app} = \frac{Flux}{C_t \times A}$$

where C_t is the donor compartment concentration at time 0, and *A* is the surface area of the Transwell filter (1.1 cm^2) and flux the slope of dye concentration over time.

Effective permeability (P) was determined using equation 6:

6) $$\frac{1}{P} = \frac{1}{P_{app}} - \frac{1}{P_m}$$

where P_m is the dye's permeability across a membrane without an organotypic slice.

Results

Arachnoid cells labelled with CellTracker showed consistent and uniform growth into the brain slice (Figure 1). Initially, cells were observed to be scattered uniformly on the brain surface with some minor clustering but without monolayer formation. Arachnoid cells penetrated into the brain slice within 2-4 days following seeding. No pattern of clusters or specific formations were observed within the brain slice. However, cells were regularly observed around blood vessels (Figure 2A). The cells exhibited a range of morphologies, from bipolar and tripolar spindles (Figure 2B) during the migration phase to a more robust polygonal shape as cells became established. Processes with lengths of greater than 100μ were occasionally seen and orientation of the processes were similar to that seen in the native tissues (rat and human cultures).[15,16]

The growth phase occurred between day 2 and day 7. A growth constant of k = 0.023 was used corresponding to a doubling time of 30.4 hours (Figure 3A). No significant change in apoptosis occurred within the first 10 days of growth when compared to arachnoid cells grown on culture plates (Figure 3B), indicating total arachnoid cell growth was not diminished by apoptosis during the acute phase and that cells mimicked 2 dimensional cultures. Figure 4 shows gradual increased arachnoid growth and a consistent pattern of minimal apoptosis throughout the experimental time periods.

Brain slices grown with arachnoid cells had significantly less indigo carmine concentration in receiver compartments than brain slices grown with fibroblasts and brain slices alone in samples taken after 2 hours (P<0.05 repeated measures ANOVA) (Figure 5). A curve was fitted to the data and the diffusion coefficient for Indigo Carmine calculated as 8.5 (±0.8) × 10^{-7} cm^2/s. Determining the transport of water is clinically important given that edema is prevalent in so many pathologic conditions. With a 4cm water pressure gradient, a higher volume of water passed through brain slices with no arachnoid cells present after 3 hours compared to brain slices with arachnoid cells (P<0.05 one way ANOVA). An 8 cm water pressure gradient showed no significant difference in flux between brain slices with and without arachnoid cells after 2 hours (P=0.29, one way ANOVA) (Figure 6). Tight junctions were observed around arachnoid cell populations throughout the brain slice (Figure 7).

When molecules are too large to cross a membrane by diffusion, there are other methods to accomplish their transport into or out of the cell. The use of large dextran molecules can lead to information as to the role of inter-cellular transport channels. However, figure 8 showed little difference in FITC labelled Dextran permeability. There was no significant difference of transport between brain slices with and without arachnoid cells. Nevertheless, significantly higher permeabilities were recorded with dextran 10

kDa and 40kDa compared to dextran 70kDa and 150kDa (P<0.05 one way ANOVA), with an apparent size differential break between 40kDa and 70 kDa for both organotypic slice and organotypic slice with arachnoid cells.

Discussion

Arachnoid granulations and protrusions are typically located within extra-parenchymal venous sinuses.[17-19] However, this study analyzed the role of arachnoid cells that has invaginated deep into brain parenchyma. These arachnoid tissues have the same origins as the pia, and while the pia is densely adherent to the brain surface they do not form barriers,[20] whereas arachnoid cells that penetrate into the brain may be important in transport and barrier formation. As they follow Virchow Robin spaces, arachnoid line blood vessels with other endothelial cells and form part of the blood brain barrier to the brain parenchyma.[21] To study these cells in this location is exceedingly difficult. The isolation of arachnoid cells from this location would take the cells out of its natural environment and is currently impossible. As the cells serve as a liaison between the endovascular space and the parenchyma, their role would require study in close proximity to native neural tissues such as astrocytes and neurons. We have used an organotypic culture model because it maintains the microarchitecture of the natural brain.

Organotypic brain slice culture models have proven useful in investigating cellular and molecular processes of the brain *in-vitro,*[22-25] but *these* constructs have only been used to study CSF dynamics and barrier formation in a limited fashion (i.e. survival of cells, neurotoxicity assays, vascular damage, rate of drug delivery, protein regulation). Their advantage includes mimicking an environment not possible within in-vitro monolayer systems.[26] Other advantages include direct observation of cell to cell contacts in their normal positions and duplication of the microenvironment surrounding the relevant cells. Reproduction of physiologic chemical gradients is possible given the anatomic compartmentalization with defined flow vectors and pressure gradients found in pathologic conditions, but with clear compartmentalization of tissue.[24,27,28]

The survival of cells grown on brain slice cultures can vary greatly among tissues and over time.[22] We found the arachnoid cells grew readily into brain slices and reached a population limit around day 10. The majority of cells were located within 100 um of the brain surface, with minimal apoptosis after 10 days. Arachnoid cells had normal appearing polygonal morphologies, consistent cell process numbers, and maintained their phenotype in the three-dimensional organotypic environment. Though dense patterns or specific formations were not observed, arachnoid cells were regularly found around blood vessels,

similar to what is found in-vivo.[18,19] As CSF is reabsorbed into venous sinus blood via arachnoid granulations it is comprehensible that arachnoid cells gravitate towards these areas and may be supported by vasculature endothelial growth factors (VEGF). In-vitro studies have shown the VEGF family to stimulate growth, migration, sprouting of neuronal cells[29] and has demonstrated to be a neuroprotectant in models of ischemic/hypoxic injury in the central nervous system.[30] Enhancement of VEGF in future organotypic studies may help determine the arachnoid response to different stimuli. In this study the limited arachnoid saturation into deeper portions of the brain slice may be a consequence of competitive interactions with other neuroectodermal cells,[31] apoptosis, or environmental factors like limited oxygen availability[32,33] or gas exchange.

In the majority of organotypic models the restriction of paracellular transport can be governed by a variety of mechanisms and components including: cell height, paracellular space tortuosity, tight junctions, gap junctions,[10,34,35] and neuronal and glial-endothelial cell relationships.[36-38] In this study, the extracellular component of the arachnoid CSF sink appeared to be important in the transport of fluid and small molecular weight molecules. Brain slices cultured with arachnoid cells permitted less dye to pass through tissue than organotypic slices without arachnoid cells, presumably by forming tight junctions with neighboring glial cells, neurons, and astrocytes. Previous in-vivo analysis of human granulations and cells grown on 2D membranes and 3d scaffolds have shown tight junction formation by electron microscopy and immunostaining within seven days of culturing.[10,15] From our tracer, small molecule, and radioactive water studies,[11,12] it is clear that the presence of arachnoid cells also impacted the movement of water through brain parenchyma. As indicated by our flux determination the effect was marked after a time period of 2 hours required for stabilization. Our model was constrained to low pressures as the impact of arachnoid was not visible once the pressure of 8 cm had been reached. It is possible that cytologic barriers, such as gap junctions and tight junctions are overwhelmed by bulk flow when pressures exceed this mark. As a consequence, diffusion of molecules should occur in a compact parenchyma, as it happens in-vivo.[5,19] The variable pressure gradients used in our system could be a useful tool to assess how brain tissue permeability changes through time and among different environmental factors. Determining the transport of water at different pressures is clinically important given that edema is prevalent in so many pathologic conditions.

Although organotypic cultures are powerful tools for studying paracellular transport, it is important to be aware of their limitations. One drawback to organotypic experimentation includes the risk of hypoxia,

which does not mimic the brain's natural environment. While several parameters influence oxygen diffusion, such as slice thickness, matrix stiffness and metabolic activity,[39,40] our organotypic brain slice tissue model represents a solid model for short to medium-term barrier and transport assays. However, mass transport did not appear to be altered by the presence of arachnoid cells. Directly comparing this with monolayers is difficult because of the underlying presumptions of mannitol permeability, and trans-epithelial electrical resistance (TEER) studies used in the Transwell model cannot be used as a surrogate for barrier formation in brain slices.[41] We show that the molecular weight profiles match what is expected for barrier formation with a cutoff of around 40 kDa, indicating the parenchyma volumetrically still maintains barrier properties throughout. Our data support the concept of the brain as porous media and have shown that intra-parenchymal-arachnoid can affect its transport physiology. Like blood-brain barrier cells and choroid plexus cells, arachnoid cells can express drug transport proteins and likely contribute to the blood-CSF drug permeation barrier.[2] We have demonstrated that arachnoid cells appear to preferentially effect bulk flow over mass transport of material in barrier defined regime. Future work using our organotypic model should include further development of mass transport assays.

In summary, we provide evidence that arachnoid cells grown in organotypic slices possess similar characteristics to what is found in-vivo. We have demonstrated that diffusion is altered in the presence of arachnoid and that changes in pressure can modify arachnoid behavior at the brain-leptomeningeal interface. This model has applications to model a number of important diseases involved in fluid and solute transport at the brain-CSF interface, including hydrocephalus, subarachnoid hemorrhage, traumatic brain injury, brain tumors, stroke, and Alzheimer's disease.

DECLARATIONS:

Ethics approval and consent to participate

All applicable international, national, and/or institutional guidelines for the care and use of animals were followed.

Competing interests

The authors declare that they have no competing interests

Funding

The work is supported by the VA Merit Review Grant #1I01BX001657-01

References:

1. Hansen EA, Romanova L, Janson CG, Lam CH. The effects of blood and blood products on the arachnoid cell. *Exp Brain Res* 2017;235(6):1749-1758.
2. Yasuda K, Cline C, Vogel P, et al. Drug transporters on arachnoid barrier cells contribute to the blood-cerebrospinal fluid barrier. *Drug Metab Dispos* 2013;41(4):923-931.
3. Kwee, RM, Kwee TC. Virchow-Robin Spaces at MR Imaging. *Radiographics* 2007;27(4):1071-1086.
4. Adeeb N, Mortazavi MM, Tubbs RS, Cohen-Gadol AA. The cranial dura mater: a review of its history, embryology, and anatomy. *Childs Nerv Syst* 2012;28(6):827-37.
5. Brinker T, Stopa EG, Morrison JF, Klinge PM. A new look at cerebrospinal fluid circulation. *Fluid Bar CNS* 2014;11(1):10-10.
6. Bacyinski Andrew, Maosheng X, Wei W, and Jiani Hu. The Paravascular Pathway for Brain Waste Clearance: Current Understanding, Significance and Controversy. *Front Neuroanat* 2017;11:101.
7. Morris AW, Sharp MM, Albargothy NJ, et al. Vascular basement membranes as pathways for the passage of fluid into and out of the brain. *Acta Neuropathol* 2016;131(5):725-736.
8. Hladky SB, Barrand MA. Mechanisms of fluid movement into, through and out of the brain: evaluation of the evidence. *Fluids Bar CNS* 2014; 11 (1): 26-26.
9. Lam CH, Hansen EA, Hubel A. Arachnoid cells on culture plates and collagen scaffolds: phenotype and transport properties. *Tissue Eng Part A* 2011;17(13-14):1759-1766.
10. Holman DW, Kurtcuoglu V, Grzybowski DM. Cerebrospinal fluid dynamics in the human cranial subarachnoid space: an overlooked mediator of cerebral disease. II. In vitro arachnoid outflow model. *J R Soc Interface R Soc* 2010;7:1205–1218.
11. Lam CH, Hansen EA, Hall WA, Hubel A. Application of transport phenomena analysis technique to cerebrospinal fluid. *J Neurosurg Sci* 2013;57(4):317-326.
12. Lam CH, HansenEA, Janson C, Bryan A, Hubel A. The Characterization of arachnoid cell transport II: paracellular transport and blood-cerebrospinal fluid barrier formation. *Neuroscience* 2012;222:228-38.
13. Ichikawa-Tomikawa N, Sugimoto K, Satohisa S, Nishiura K, Chiba H. Possible involvement of tight junctions, extracellular matrix and nuclear receptors in epithelial differentiation. *J Biomed Biotechnol* 2011;2530-48.
14. Janson C, Romanova L, Hansen E, Hubel A, Lam C. Immortalization and functional characterization of rat arachnoid cell lines. *Neuroscience* 2011;177:23-34.
15. Grzybowski, DM., Holman DW, Glimcher SA. Ultrastructural study of the permeability of in-vitro and ex-vivo human models of human arachnoid granulation CSF outflow pathway. *Cerebrospinal Fluid Res* 2007;(1-2) 4 (1): 1-2.
16. Rutka JT, Giblin J, Dougherty DV, McCulloch JR, DeArmond SJ, Rosenblum ML. An ultrastructural and immunocytochemical analysis of leptomeningeal and meningioma cultures. *J Neuropathol Exp Neurol* 1986;45(3):285-303.
17. Sakka L, Coll G, Chazal J. Anatomy and physiology of cerebrospinal fluid. *Eur Ann Otorhinolaryngol Head Neck Dis* 2011;128(6):309-316.

18. Leach JL, Jones BV, Tomsick TA, Stewart CA, Balko MG. Normal appearance of arachnoid granulations on contrast-enhanced CT and MR of the brain: differentiation from dural sinus disease. *AJNR Am J Neuroradiol* 1996;17(8):1523-1532.
19. Carpenter, Malcolm. 1991. Core text of neuroanatomy. Williams & Wilkins.
20. Engelhardt B, Vajkoczy P, Weller RO. The movers and shapers in immune privilege of the CNS. *Nat Immunol* 2017;18(2):123-131.
21. Ek, CJ, Dziegielewska, KM, Stolp H, Saunders NR. Functional effectiveness of the blood-brain barrier to small water-soluble molecules in developing and adult opossum (Monodelphis domestica). *J Compar Neurolog* 2006;*496*(1),13–26.
22. Humpel C. Organotypic brain slice cultures: A review. *Neuroscience* 2015;305:86-98.
23. Drexler B, Hentschke H, Antkowiak B, Grasshoff C. Organotypic cultures as tools for testing neuroactive drugs - link between in-vitro and in-vivo experiments. *Curr Med Chem* 2010;17(36):4538-4550.
24. Morin-Brureau M, De Bock F, Lerner-Natoli M. Organotypic brain slices: a model to study the neurovascular unit micro-environment in epilepsies. *Fluids Barriers CNS* 2013;10(1):11.
25. Kim H, Kim E, Park M, Lee E, Namkoong K. Organotypic hippocamal slice culture from the adult mouse brain: A versatile tool for translational neuropsychopharmacology." *Prog Neuropsychopharmacol Biol Psychiatry* 2013;41:36–43.
26. Czupalla, CJ, Liebner S, Devraj K. In vitro models of the blood-brain barrier. *Methods Molec Biol* 2014;1135:415-437.
27. Nag S, Kapadia A, Stewart DJ. Review: molecular pathogenesis of blood-brain barrier breakdown in acute brain injury. *Neuropathol Appl Neurobiol* 2011;37(1):3-23.
28. Daneman R, Prat A. 2015 The Blood–Brain Barrier. Cold Spring Harbor Perspectives in Biology 2015; 7 (1).
29. D'Amore PA. Vascular endothelial cell growth factor-a: not just for endothelial cells anymore. *Am J Pathol* 2007 Jul;171(1):14-8.
30. Gora-Kupilas, K, Josko J. The neuroprotective function of vascular endothelial growth factor (VEGF). *Folia Neuropathologica* 2005;43:31-39.
31. Ozdil B, Güler G, Acikgoz E, Kocaturk DC, Aktug H. The effect of extracellular matrix on the differentiation of mouse embryonic stem cells. *J Cell Biochem* 2020;121(1):269-283.
32. Ramírez MÁ, Pericuesta E, Yáñez-Mó M, Palasz A, Gutiérrez-Adán A. Effect of long-term culture of mouse embryonic stem cells under low oxygen concentration as well as on glycosaminoglycan hyaluronan on cell proliferation and differentiation. *Cell Prolif* 2011;44(1):75-85.
33. Chopard RP, Brancalhão RC, Miranda-Neto MH, Biazotto W. "Arachnoid granulation affected by subarachnoid hemorrhage." *Arq Neuropsiquiatr* 1993;51:452–456.
34. Harhaj NS, Antonetti DA. Regulation of tight junctions and loss of barrier function in pathophysiology. *Int J Biochem Cell Biol* 2004;36(7):1206-1237.
35. Stoppini L, Buchs PA, Muller D. A simple method for organotypic cultures of nervous tissue. *J Neurosci Methods* 1991;37: 173–182.
36. Tontsch U, Bauer HC. Glial cells and neurons induce blood-brain barrier related enzymes in cultured cerebral endothelial cells. *Brain Res* 1991;539(2):247-53.

37. Duport S, Robert F, Muller D, Grau G, Parisi L, Stoppini L. An in vitro blood-brain barrier model: cocultures between endothelial cells and organotypic brain slice cultures. *Proc Natl Acad Sci U S A* 1998;95: 1840–1845.
38. Weller RO, Sharp MM, Christodoulides M, Carare RO, Møllgård K. The meninges as barriers and facilitators for the movement of fluid, cells and pathogens related to the rodent and human CNS. *Acta Neuropathol* 2018;135(3):363-385.
39. Naipal KA, Verkaik NS, Sánchez H, van Deurzen CH, den Bakker MA, Hoeijmakers JH, Kanaar R, Vreeswijk MP, Jager A, van Gent DC. Tumor slice culture system to assess drug response of primary breast cancer. *BMC Cancer* 2016;*16*: 78.
40. Wang Q, Andreasson K. The organotypic hippocampal slice culture model for examining neuronal injury. *J Vis Exp* 2010;(44):2106.
41. Vernon H, Clark K, Bressler JP. In vitro models to study the blood brain barrier. *Methods Mol Biol* 2011;758:153-168.

Figures

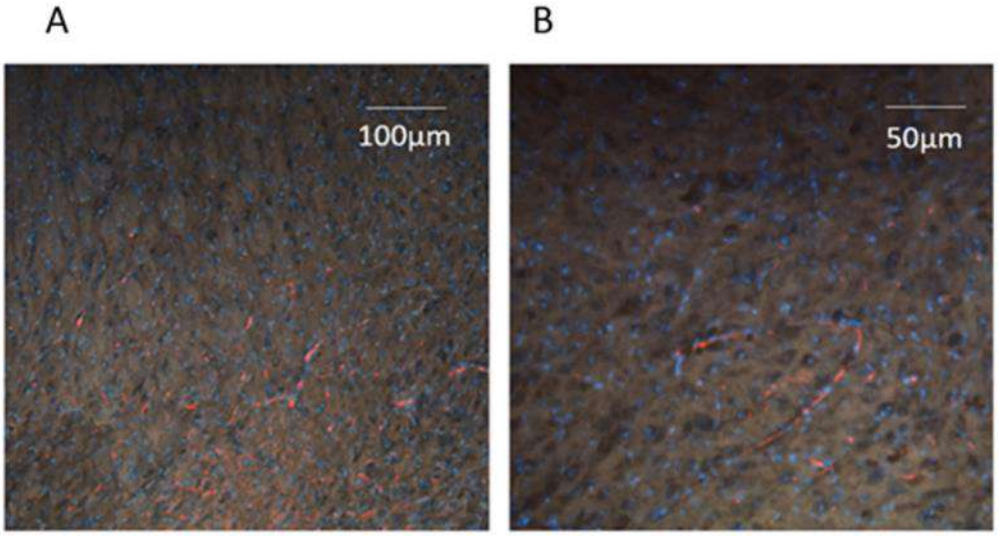

Figure 1. Brain slice cultured at 7 days with the addition of labelled arachnoid cells (Red). Nuclear staining is with DAPI. Image was taken at 100 µm depth using a Biorad MRC-1024 single photon confocal microscope 1024 merged with brightfield (Biorad Cell Science, UK). (A taken at 10x B. taken at 20x).

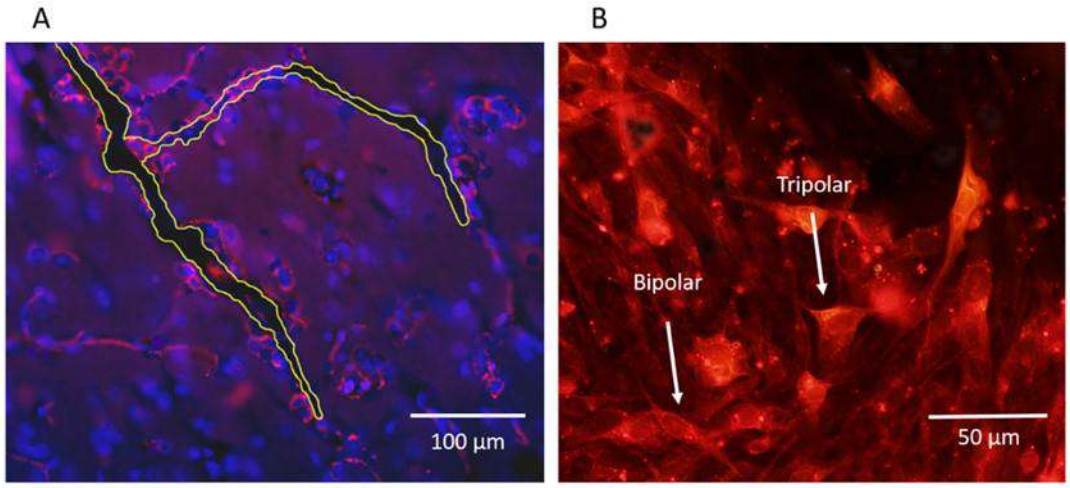

Figure 2. Brain slice cultured at 7 days with the addition of labelled arachnoid cells (red) including nuclear staining DAPI (blue) (A). Yellow outline indicates blood vessels within the brain slice, with arachnoid growing in close proximity. Image was taken at 40x and 100 µm depth. Panel B shows brain slice cultured at 4 days showing bipolar and tripolar morphology of arachnoid cells (red). Image was taken at 60x and 50 µm depth using a Biorad MRC-1024 single photon confocal microscope 1024 (Biorad Cell Science, UK).

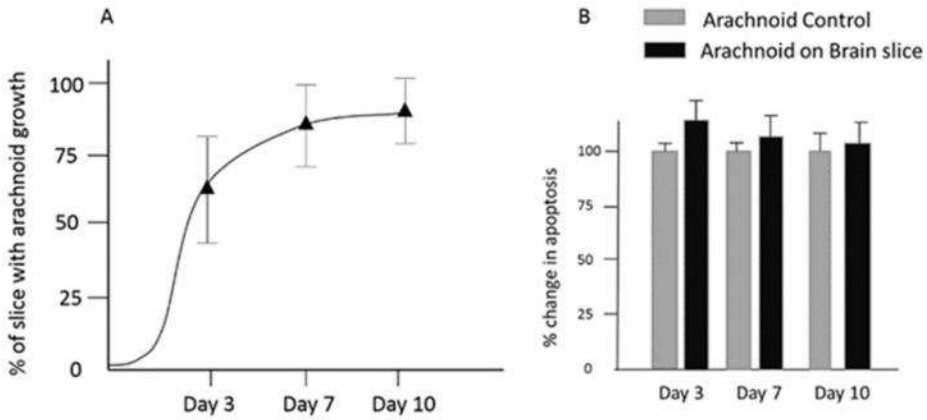

Figure 3. Growth of arachnoid cells on organotypic brain slices. The arachnoid cells grew in brain slices with cell populations eventually reaching a limiting size at approximately 10 days following seeding (A). Limited apoptosis in brain slices was observed over 10 days with no significant difference between organotypic slices and arachnoid cell controls (one-way ANOVA P=0.34) (B).

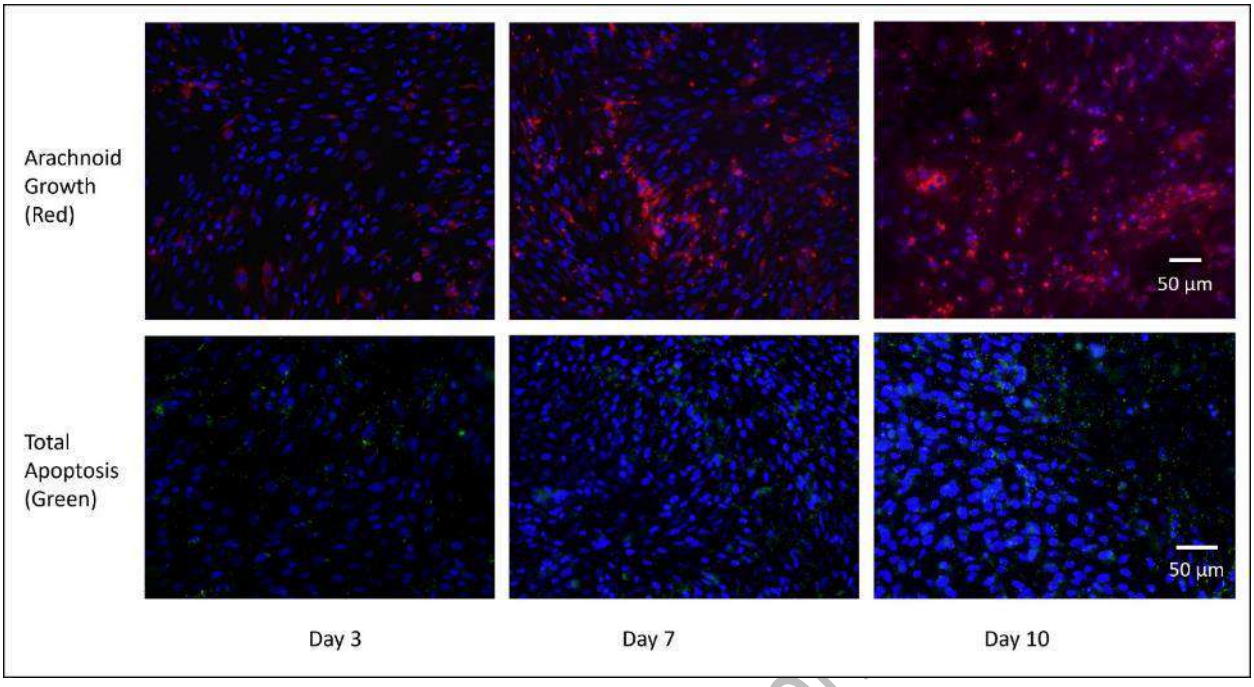

Figure 4. Arachnoid (red) across the top line shows increased growth within brain slices over 10 days. Consistently low apoptosis (green) across the bottom row was recorded throughout the same growth period. Image was taken at 10x at a 150 µm depth using a Biorad MRC-1024 single photon confocal microscope 1024 (Biorad Cell Science, UK).

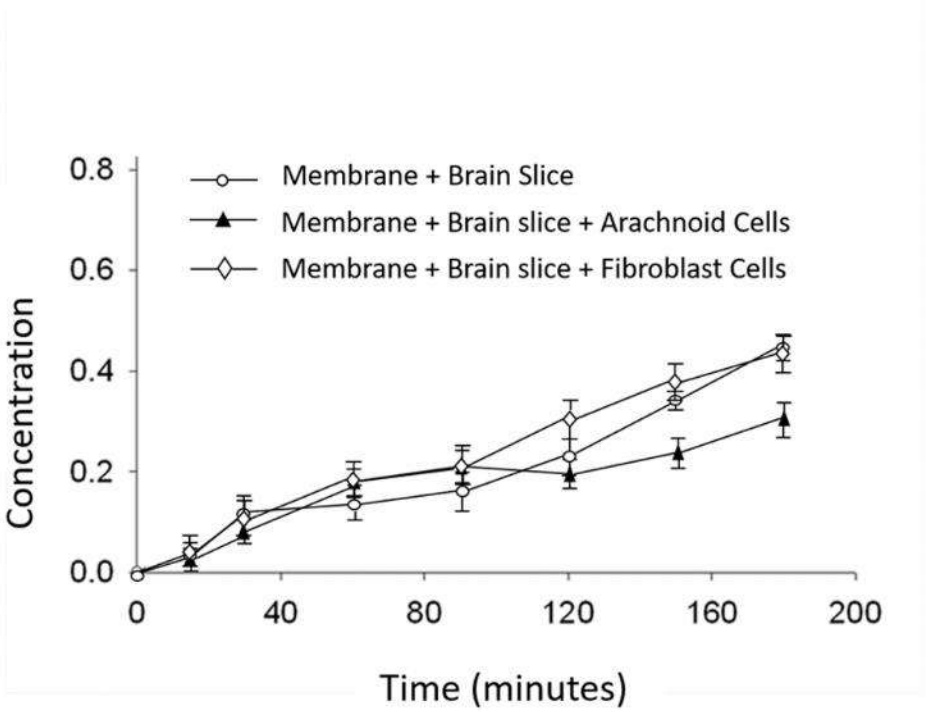

Figure 5. Cells grown on Transwell membranes were allowed to reach confluency which occurred at approximately 7 days in culture. Membranes were placed in the diffusion chamber and concentration of indigo carmine dye in the receiver compartment recorded over time. By 2.5 hours, the concentration of indigo carmine in brain slices grown with arachnoid was significantly less than in brain grown with fibroblast and brain slices alone. By hour 3, the concentration of Indigo Carmine in controls was almost double that of concentration in receiver compartments with brain slices.

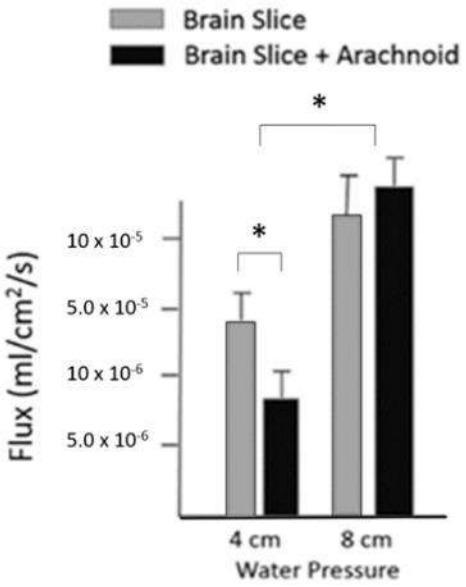

Figure 6. Cells grown on transwell membranes were allowed to reach confluency. Chamber experiments under pressure conditions showed a significant increase in flux at 4 cm water pressure where brain slices did not contain arachnoid cells.

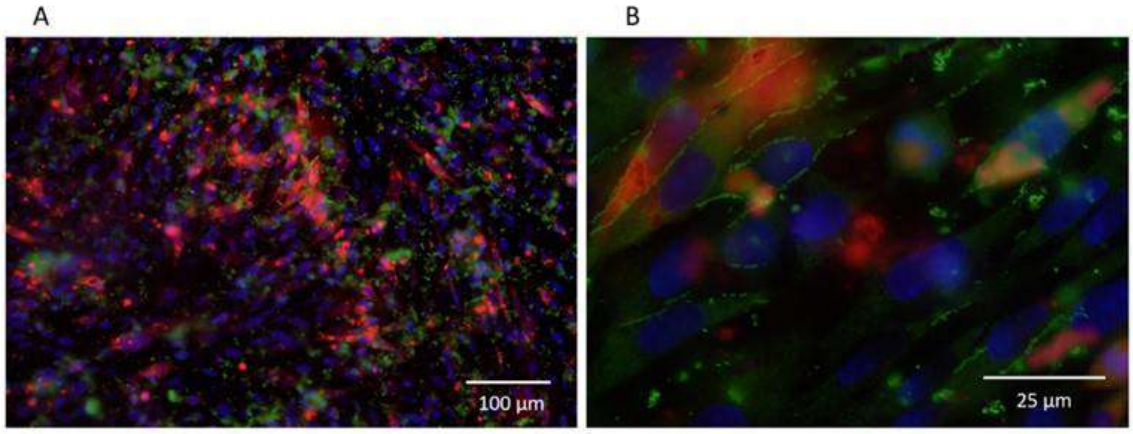

Figure 7. Brain slices were cultured for 7 days to monitor tight junction formation. Claudin-5 staining (green) and labelled arachnoid (red). Taken at 100 µm depth at 10x (A) and 60x (B) using a Biorad MRC-1024 single photon confocal microscope 1024 (Biorad Cell Science, UK).

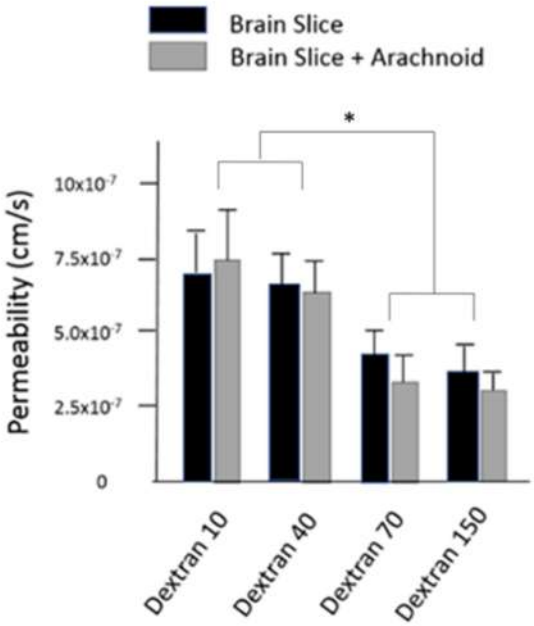

Figure 8. Brain slices were cultured for 7 days, the permeability of FITC labelled dextran (10, 40, 70 and 150 KDa) across brain slices with and without the addition of arachnoid cells. Significantly higher permeabilities were recorded with dextran 10 kDa and 40kDa compared to dextran 70kDa and 150kDa (P<0.05 one way ANOVA).